



Seasonally frozen soil modifies patterns of boreal peatland wildfire vulnerability

Simon J Dixon^{1*}; Max C Lukenbach²; Nicholas Kettridge¹; Kevin J Devito³; Richard M
Petrone⁴; Carl A Mendoza²; J Michael Waddington⁵

¹ School of Geography, Earth and Environmental Sciences, University of Birmingham,
Edgbaston, Birmingham, B15 2TT, UK.

² Department of Earth and Atmospheric Science, University of Alberta, Edmonton, AB, T6G
2E3, Canada

³ Department of Biological Sciences, University of Alberta, Edmonton, AB, T6G 2E9,
Canada

⁴ Department of Geography and Environmental Management, University of Waterloo,
Waterloo, ON, N2L 3G1, Canada

⁵ School of Geography and Earth Sciences, McMaster University, Hamilton, ON, L8S 4K1,
Canada

* - Corresponding Author: s.j.dixon@bham.ac.uk



1 **Abstract**

2 Peatlands play a vital role in the global carbon cycle, acting as one of the most important
3 global carbon sinks. However, an understanding of their environmental processes,
4 particularly in relation to a changing climate, remains incomplete. In particular, the role
5 seasonal ice or frost layers play in altering spring water balance, and thus vulnerability to
6 deep smoldering combustion during wildfire is not fully understood. Continental boreal
7 peatlands are characterized by periodic wildfire disturbance, which releases carbon, but can
8 also inhibit short-term peat productivity and carbon sequestration as the peatland recovers,
9 with recovery timescales linked to the severity or depth of burning. The presence of seasonal
10 frost layers coincides with drier spring conditions and an enhanced risk of wildfire. Two-
11 dimensional numerical modelling was conducted using HYDRUS-2D, a variably saturated
12 flow model, to simulate water balance in the vadose zone and assess vulnerability to fire
13 during prolonged rain free periods in the presence of continuous and discontinuous frost.
14 Our results show there is a lack of horizontal water transfer which increases spatial
15 variability in water balance and leads to pronounced heterogeneity in the risk of smoldering
16 combustion and the potential for deep combustion at hummock-hollow interfaces. Peatlands
17 are broadly divided into areas which are characterized by a dry near-surface and high water
18 contents at depth (water conserving), and those with a wetter near-surface, but
19 comparatively lower water contents at depth (productive). Those areas with dry near-
20 surfaces will be more vulnerable to wildfire and characterize around 50% of hummocks and
21 25% of hollows. In the presence of a seasonal frost layer productive peat layers in hollows
22 will show substantial drying out due to the frost layer disconnecting the surface from the
23 water table; this approximately doubles the proportion of hollows vulnerable to wildfire.
24 Breaks in the frost layer allows areas to maintain hydrological connectivity to a falling water
25 table, but this connectivity is limited in lateral extent and can drive further spatial
26 heterogeneity in vulnerability to wildfire ignition in the weeks when the frost layer begins to
27 thaw.



28 1. Introduction

29 Peatlands are an important global carbon sink (Frolking and Roulet, 2007;Gorham, 1991),
30 accounting for up to 30% of the total soil carbon pool despite covering 3% of the global land
31 surface (Gorham, 1991;Smith et al., 2004;Yu et al., 2010). Wildfire is the largest natural
32 disturbance impacting northern peatlands (Stocks et al., 2002) and is increasing in areal
33 extent (Turetsky et al., 2002). From 1960 to 1990, the annual area burnt across boreal North
34 America doubled (Kasischke and Turetsky, 2006), and is projected to increase 118% by 2100
35 (Flannigan et al., 2005). Peatland carbon stocks are generally resilient to wildfire, returning
36 to a net carbon sink approximately 13 years post-fire (Wieder et al., 2009). However, there
37 are concerns that increased drying under future climates (Roulet et al., 1992) will increase
38 wildfire severity (Turetsky et al., 2011), potentially transforming peatlands into a net carbon
39 source (Turetsky et al., 2004) and leading to the long term degradation of their carbon stocks
40 (Kettridge et al., 2015b).

41 Smouldering is the dominant form of combustion of peatland carbon stocks (Benscoter et al.,
42 2011), with burn depths typically ranging from 0.05 – 0.10 m (Benscoter and Wieder,
43 2003;Lukenbach et al., 2015b;Shetler et al., 2008;Hokanson et al., 2016). Burn severity and
44 smouldering (measured as depth of burn, DOB) are strongly controlled by the gravimetric
45 water content (GWC) through the peat profile (Prat-Guitart et al., 2016;Benscoter et al.,
46 2011;Lukenbach et al., 2015b). The GWC of peat is a function of water content and peat
47 density, GWC thus determines the balance between a continued energy source to sustain
48 combustion, produced by the burning of peat, and the energy sink (Benscoter et al.,
49 2011;Prat-Guitart et al., 2016). Where GWC is low, small amounts of energy from the
50 combustion of overlying or adjacent peat are sufficient to drive off water held within the
51 peat to propagate smouldering (Benscoter et al., 2011). Therefore, patterns of peat moisture
52 content and bulk density, which control peat GWC, are crucial to determining patterns of
53 smouldering during peatland wildfire.

54 Complex interactions between peat hydrophysical properties (*e.g.* bulk density, unsaturated
55 hydraulic conductivity) and atmospheric water demand control the distribution of peat
56 moisture contents in the vadose zone, thereby influencing GWC and peat burn severity.
57 However, boreal and sub-arctic peatlands are also characterised by pronounced seasonality.



58 During winter, snow typically covers peat soils in many places that are either completely
59 frozen, or have frost lenses below the surface. Herein, we refer to this seasonally frozen soil
60 as a “frost layer”. Following spring snowmelt, frost layers thaw unevenly producing a
61 heterogeneous landscape composed of frost free and frozen profiles (Petroni et al., 2008). In
62 parts of Alberta this prolonged period of frost thawing can last into the summer months
63 due to the insulating effect of the near-surface peat, potentially decoupling peatland vadose
64 zone processes from the saturated zone (Thompson and Waddington, 2013). Decoupling
65 may prevent water lost through evapotranspiration being replenished by limiting the
66 upward capillary flow from the water table, inducing substantial drying of the near-surface.
67 This enhanced drying would coincide with a spring period of heightened wildfire risk in
68 continental boreal peatlands (Stocks et al., 2002) and may enhance early season wildfire burn
69 severity (Turetsky et al., 2011).

70 Seasonal ice dynamics in peatlands not only have the potential to impact carbon loss during
71 combustion, but may also influence the ecological trajectory post disturbance. Wildfire burn
72 severity directly impacts peatland post-fire ecological recovery (Lukenbach et al., 2016),
73 impacting the ability of the peat forming mosses to re-establish. Specifically, the interaction
74 between pre-fire species cover and burn severity have a large influence on post-fire water
75 availability (Lukenbach et al., 2015a, 2016), thereby playing a large role in the recolonization
76 of peat-forming species. Therefore, if seasonal frost layers influence peat burn severity by
77 altering GWCs at the time of wildfire it could change short-term carbon cycling in these
78 landscapes.

79 In this study, we characterise near-surface frozen soil thaw dynamics within an unburned
80 boreal peatland at a high spatial resolution. We simulate the control of this frozen layer on
81 near-surface peat moisture dynamics using HYDRUS 2D, with specific emphasis on the
82 ability of frozen layer to disconnect saturated water stores from the near surface. We assess
83 how this control is modified by gaps within the frost layer, and consider the associated
84 impact on early season wildfire severity and post-fire peatland recovery. The study has three
85 objectives, to; i) use field measurements to characterise changes in the spatial extent of
86 frozen soil at high spatial resolution within a northern peatland from snowmelt until the
87 disappearance of frost, ii) explore how hydraulic properties and frost layer continuity



88 interact to drive vertical and lateral transfers of water during prolonged rain free periods of
89 high fire risk, iii) explore how spatial variability in hydraulic properties, peatland
90 microforms and frost layers interact to induce spatial variability in GWC and associated
91 smouldering severity during the exceptionally dry periods which precede wildfires.

92 2.Methods

93 2.1 Study site

94 Measurements were undertaken within a peatland (55.8° N, 115.1° W) within the lacustrine
95 clay region of the Utikuma Lake Research Study Area (URSA) in the Boreal Plains ecotone
96 (Devito et al., 2012), which has not burned since ~1935. It is characterized by hummock
97 hollow microtopography, with ground layer vegetation consisting of *S. fuscum*, *S.*
98 *angustifolium* and *feather moss*. Vascular vegetation cover includes *Ledum groenlandicum*,
99 *Rubus chamaemorus*, *Maianthemum trifolia*, *Vaccinium oxycoccus* and *V. vitus-idea*, and the
100 canopy is comprised of black spruce (*Picea mariana*) with a basal area of 11 m² ha⁻¹ and an
101 average height of 2.3 m. For a full site description see Thompson and Waddington (2013) .

102 2.2 Field Data

103 To examine spatiotemporal variations in depth to ice (objective *i*), depth to ice was measured
104 bi-weekly along a 50 m transect every 0.25 m (to a maximum depth of 0.5 m) through the
105 initial stages of the growing season (following snow melt) until no ice was detected (10th
106 May to 22nd July). Depth to ice was measured by pushing a metal rod through the peat
107 profile until solid frozen soil was detected. Near-surface peat moisture content was also
108 measured with a Delta-T theta probe at each point on the transect. Each sampling location
109 was also classified as a hummock or hollow, and the species cover was noted. Further the
110 relative elevation of each position along the transect was determined using a hose level
111 gauge.

112 2.3 Numerical Modelling

113 2.3.1 Model Description

114 Simulations were conducted using Hydrus-2D (Šimůnek et al., 1999), a two-dimensional
115 finite element model for simulating water flow in a variably saturated and unsaturated
116 medium with the model domain, discretised as a triangular grid. The governing flow
117 equation is a modified version of the Richard's equation:



118

$$\frac{\partial \theta}{\partial t} = \frac{\partial}{\partial x_i} \left[K \left(K_{ij}^A \frac{\partial h}{\partial x_j} + K_{ij}^A \right) \right] - S, \quad 1$$

119

120 where θ is water content, K is hydraulic conductivity, h is pressure head and S is the sink
121 term. Water retention is characterised by the Van Genuchten (1980) model:

$$\theta(h) = \left\{ \theta_r + \frac{\theta_s - \theta_r}{(1 + (a|h|)^n)^m \theta_s} \right\} \quad h < 0 \quad h \geq 0, \quad 2$$

122

123 and:

$$m = 1 - \frac{1}{n} \quad n > 1, \quad 3$$

124

125 where $\theta(h)$ is soil water retention as a function of the pressure head h , θ_r and θ_s are the
126 residual water content and saturated water content for the media respectively, a is an
127 empirical parameter related to the inverse of air entry pressure (m^{-1}) and n is an empirical
128 parameter for the pore size distribution. Unsaturated hydraulic conductivity (K) is a
129 function of saturated hydraulic conductivity (K_s) and pressure head:

$$K(h) = K_s S_e^L \left(1 - \left(1 - S_e^{1/m} \right)^m \right)^2 \quad h < 0 \quad 4$$

$$K(h) = K_s, \quad \text{when } h \geq 0$$

$$S_e = \frac{\theta - \theta_r}{\theta_s - \theta_r}$$

130

131 S_e is the effective saturation and L is a dimensionless pore tortuosity parameter (Simunek et
132 al., 1998).

133 2.3.2 Modelling domain

134 Two modelling domains were constructed to address objectives *ii* and *iii* (regular and
135 microtopography domains). The model domain for objective *ii* comprised a two-dimensional
136 grid in the xz plane, 5 m wide and 2 m thick, with a grid discretisation of 3 mm and a
137 horizontal stretching factor of 5. During numerical simulations, it was assumed that no flux
138 occurred across frozen layers based on the very low hydraulic conductivity of frozen soil
139 (McCauley et al., 2002). This was implemented to simulate a frozen layer with zero water
140 flux, inactive cells were included within this basic model framework; these rectangular



141 geometric objects were situated at a depth of 0.15 m below the soil surface. The inactive
142 objects are 0.10 m thickness with a width specified by the modelling scenario. Grid
143 refinements are applied to points at the evaporating surface and point on the upper edge of
144 the geometry representing the frost layer; this refinement yields a finer model grid nearer
145 the atmospheric boundary and around the no flow (frozen) layer, compared to the base of
146 the grid. Moisture contents were recorded at the evaporating surface, and depths of 0.05,
147 0.10, 0.15 and 0.50 m.

148 The model domain for objective *iii* simulated a peatland microtopography sequence of
149 hummocks and hollows. The model domain was a grid in the xz plane, 5 m wide. The
150 hummock-hollow surface topography was characterised as a continuous curve from the top
151 of the hummocks to the base of the hollows. The hummock-hollow sequence had an
152 amplitude of 0.4 m and wavelength of 2 m. The model domain contains a total of 2.5
153 hummock-hollow sequences. Therefore, the depth from the hummock and hollow surface to
154 the base of the model domain was 1.4m and 1.0 m, respectively.

155 **2.3.3 Boundary and initial conditions**

156 The initial conditions of the regular model domain were set assuming an equilibrium
157 pressure head through the peat profile. For the planar surface model domain, the starting
158 water table (zero pressure head) was set at a depth of 0.05 m below the evaporating surface.
159 In the case of the microtopography domain, the water table was set to a depth of 0.05 m
160 below the lowest point of the hollow. The base and sides of all model domains were set as
161 no flow boundaries and the surface as an atmospheric boundary. A time variable flux was
162 applied to the atmospheric boundary, representing the diurnal variation in
163 evapotranspiration over a 50 day modelling period, assuming no rainfall input (Dixon et al.,
164 2017). We therefore aim to model a prolonged period of potential drying which would
165 typically precede a spring wildfire. For example, within the fire prone regions of the western
166 boreal plain, Canada, between 1922 and 2007, 10% of the months of May had less than 16
167 mm of precipitation, with a minimum of 5.6 mm (Slave Lake, Environment Canada, 2017). A
168 threshold value for when surface tension inhibits evaporation (h_{CritA}) is employed. Here
169 we apply a value of 400 mb to represent vegetative stress within mosses limiting
170 evaporation (McCarter and Price, 2014). The frost layer is modelled as rectangular blocks in
171 the model domain with all edges set as no flow boundaries; we thus model the frozen layer



172 as a static part of the domain without freeze-thaw mechanics. We are therefore modelling
173 the effect of the frost layer only on disconnecting the near-surface of the model domain from
174 the deeper saturated layer. This is an exploratory modelling framework to examine the
175 impact of frost layer disconnection that does not account for the recharge effects of water
176 provided from thawing frost during the model run. The magnitude of this potential daily
177 recharge rate will be determined from observed rates of ice melt and considered in the
178 context of wider modelling assumptions, notably evaporation rate, initial moisture
179 conditions, and h_{CritA} . The modelling results should therefore be seen not in terms of
180 absolute predictions, but rather comparisons in the response, and magnitude of response,
181 between different scenarios.

182 The microtopography model was ‘spun-up’ for a period of 200 days to generate realistic
183 starting moisture conditions as using a default of equilibrium pressure heads in HYDRUS
184 generates unrealistically dry hummocks, whereas naturally hummocks are characterised by
185 relatively moist conditions a few centimetres below the surface (Benscoter and Wieder,
186 2003;Thompson and Waddington, 2013). The spin up period was applying a weekly rainfall
187 recharge to the peat surface equal to moisture lost through evapotranspiration. This spin up
188 achieved a dynamic equilibrium in water contents with a planar water table depth of
189 approximately 0.04 m from the base of the hollows and higher unsaturated moisture
190 contents in the hummocks (See supplemental material).

191 **2.3.4 Hydraulic Properties**

192 Peat hydraulic properties vary across several orders of magnitude (e.g. Hogan et al.,
193 2006;Lewis et al., 2012;Kennedy and Price, 2005;Boelter, 1965;Branham and Strack,
194 2014;Beckwith et al., 2003;Baird et al., 2008;Baird et al., 2016). These hydraulic properties
195 have a crucial control on the peatland response to evaporation (Kettridge et al., 2015a;Dixon
196 et al., 2017). However, using mean values of these properties in modelling investigations
197 fails to accurately characterise either the average response or a typical range of responses for
198 a given distribution of peat properties (Kettridge et al., 2015a;Dixon et al., 2017). Therefore,
199 we apply a distribution of hydraulic properties reported in *Dixon et al* [2017], based upon
200 field data collected by *Lukenbach et al* [2015] and *Thompson and Waddington* [2008] (Table I).



201 These data encompass a full range of peat types and properties, from centre of bogs to dense
202 margin peat areas.

203 *Kettridge et al* [2015] found that the key factors controlling whether a peat profile displayed
204 high surface tensions under evaporation (*water conserving*) or was able to maintain low
205 surface tensions during evaporative stress (*productive*) were inverse entry of air pressure (α)
206 and saturated hydraulic conductivity (K_s); where higher α and lower K_s correspond to a
207 greater likelihood of peat being water conserving under stress. In this study, due to
208 computational constraints, we conceptually define a vector through hydraulic property
209 space along the axis corresponding to α and K_s . We define three different combinations of α
210 and K_s along this vector to represent profiles across the transition from water conserving to
211 productive, and generate these values for: all peat, just hollows and just hummocks. Values
212 for α and K_s applied were the mean, and plus and minus one standard deviation from the
213 mean. Peat hydraulic properties were not varied with depth in the model. Although
214 variations in peat hydraulic properties with depth have been shown (e.g. Sherwood et al.,
215 2013), *Kettridge et al.* [2015] found only weak dependence on depth for values of α and K_s .
216 *Quinton et al* [2008] also showed that K_s is dependent on the degree of compaction and
217 decomposition, which does not necessarily show a linear relationship with depth.

218 A combination of low K_s and high α inhibit water flow and tend towards high surface
219 tension under evaporative stress; defined here as "*water conserving*". Conversely, high K_s and
220 low α readily transport water to the evaporating surface and is defined as "*productive*"
221 (Table I). We keep values of residual water content (θ_r), saturated water content (θ_s), pore
222 tortuosity (l) and n constant. For modelling scenarios with a hummock-hollow sequence we
223 further generate values for θ_s , l and n , as well as values for α and K_s (plus and minus one
224 standard deviation) for hummocks alone (Table I). It is important to note that the difference
225 in modelled hydraulic properties between hummocks and hollows is not as great as the
226 difference between the peats classified as water conserving or productive. The hydraulic
227 property type, based on the property distributions, is more important to behaviour than
228 whether the peat is a hummock or hollow. Hydraulic properties have been shown to have a
229 relationship to moss species (McCarter and Price, 2014), however this remains poorly



230 understood and more detailed field data collection is needed to parameterise these
231 relationships in numerical models.

Material	θ_r	θ_s	α	n	K_s (cm/hr)	l
Mean	0.01	0.939	1.828	1.192	18.31	-1.411
Water Conserving	0.01	0.939	2.380	1.192	16.31	-1.411
Productive	0.01	0.939	0.176	1.192	20.31	-1.411
WC Hummock	0.01	0.965	14.999	1.213	16.31	-1.411
PR Hummock	0.01	0.965	0.628	1.213	20.31	-1.411

232 Table I – hydraulic properties of peat used in the modelling scenarios and based on data in Dixon et
233 al (2017)

234 2.3.5 Modelling Design

235 To examine water flow pathways and the water balance in the presence of continuous and
236 discontinuous frost layers (Objective *ii*), four different frozen soil geometries were created
237 within the regular model domains: *i*) a continuous layer of frozen soil/frost across the model
238 width; *ii*) a 0.5 m wide gap in the centre of the frost layer; *iii*) two 0.5 m wide gaps in the
239 frost layer either side of a central 1 m wide block of frozen soil; *iv*) frost free. Mean, water
240 conserving and productive peat hydraulic properties were used to parameterise the peat
241 layers in the four model geometries, giving a total of 12 model scenarios. For Objective *iii* the
242 hummock-hollow sequence within the microtopography modelling domain was
243 parameterised with different hydraulic properties in the different microtopographical units.
244 Moving from left to right the model domain was parameterised as; a water conserving
245 hummock, a water conserving hollow, a productive hummock, a productive hollow, and a
246 water conserving hummock. The sequence ensures all four possible transitions between
247 hummock and hollow properties are represented in the model domain. The remainder of the
248 model domain was designated as having mean peat hydraulic properties.

249 2.3.6 Model Analysis

250 To assess fire severity, simulated volumetric moisture contents (VMC) were converted to
251 gravimetric water contents:

$$GWC = \frac{\theta}{\rho} \quad 5$$

252

253 where GWC is gravimetric water content and ρ is the mean density of peat for a given
254 sample.



255 A probabilistic approach is taken to estimate the likelihood that the gravimetric water
256 content of given sub-set of peat (Table I) at a given time in a model simulation is lower than
257 a threshold for smouldering wildfires ignition. A normal distribution of gravimetric water
258 contents was calculated, multiplying the VMC by the full normal distribution of peat
259 observed peat densities, given by:

$$Y \sim N(\theta\mu_p, \theta^2\sigma_p) \quad 6$$

260

261 where Y is a normal distribution with a mean of $\theta\mu_p$ and a standard deviation of $\theta^2\sigma_p$. For a
262 given gravimetric water content, in this case corresponding to the threshold for smouldering
263 (GWC=250%), the z score for a given distribution is computed as:

$$z = \frac{x - \theta\mu_p}{\theta^2\sigma_p} \quad 7$$

264

265 where x is the smouldering threshold. A probability of the gravimetric water content being
266 lower than the threshold for a given point and at a given time is expressed as a cumulative
267 normal distribution function:

$$P = \frac{\theta^2}{\sigma} \frac{1}{\sqrt{2\pi}} \int_{-\infty}^x e^{-\frac{(t - (\mu/\theta))^2}{2(\sigma/\theta^2)^2}} dt \quad 8$$

268

269 The results from Eq. (8) can then be plotted over time as a metric to indicate the probability
270 of deep smouldering as a function of gravimetric water content probability, given the
271 distribution of peat density in a given type of peat.

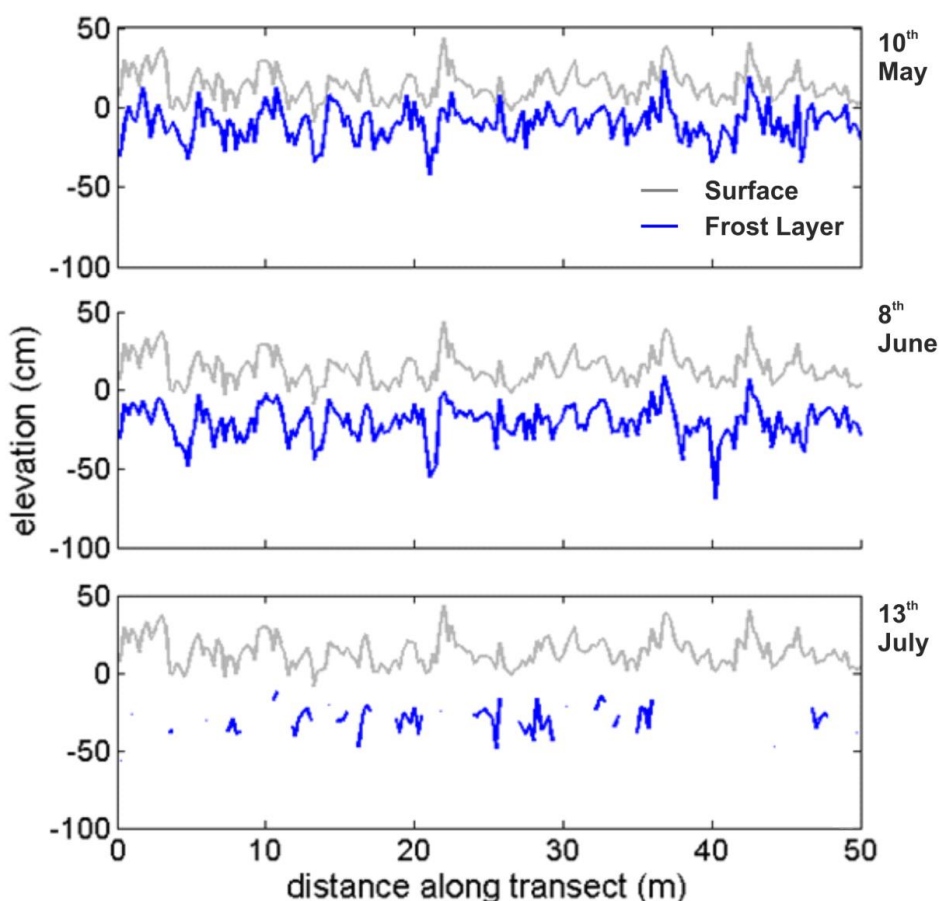
272 3. Results

273 3.1 Ice field measurements

274 Shortly after snowmelt, the frost layer largely followed the surface topography at a depth of
275 0.2-0.3 m and subsequently retreated slowly as the frozen soil nearest to the surface began to
276 thaw (Figure 1). The frozen layer eventually began to break up and disappear completely
277 over a period of five weeks from 22nd June, when the frost layer is patchy and broken though
278 in places, to 1st August, when the transect was frost free. The recession of the frozen soil
279 layer can be taken as a daily average from 10th May to the start of break up on 22nd June and
280 along with specific yield of average peat properties from our data set, gives an average daily



281 moisture recharge rate of 1.8 mm/day. During the period of frost break up, sections of frozen
282 soil 1-1.5 m in length persist whilst the frost in other areas has thawed completely. Although
283 these persistent blocks of frozen soil can be associated with either hummock or hollow
284 microtopography, the frost layer tends to begin to break up earlier in hollows than
285 hummocks. Furthermore, some of the more persistent blocks of frozen soil are in the bases of
286 hummocks. A binomial logistic regression was run on the effects of topography of the
287 presence of frost on 13th July. The Hosmer-Lemeshow test shows the model fits the data well
288 ($p=0.446$), with topography predicting presence of frost at a significance level of $\alpha=0.90$
289 ($p=0.091$).



290

291

292

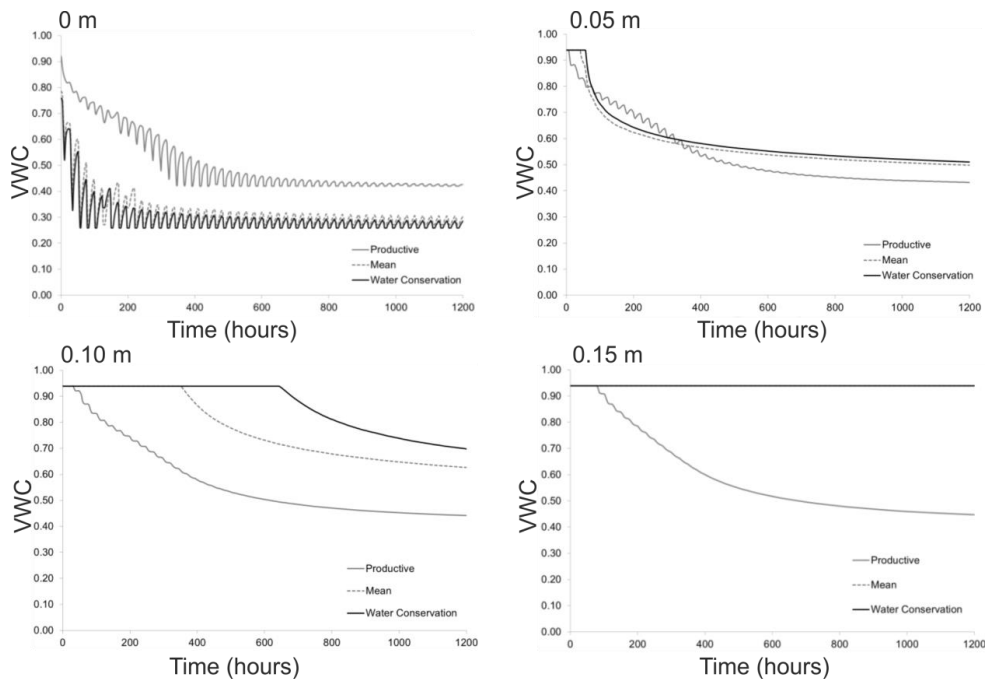
293

Figure 1 – Field measurements showing surface topography and initial depth to ice (i.e. top of the frost layer) and the breakup of ice into a discontinuous layer later in the season (note the vertical exaggeration in scale).



294 **3.2 2-D model simulations (topography excluded)**

295 Trends in water content and water movement were strongly associated with whether peat
296 hydraulic properties were “water conserving” or “productive” as well as the continuity of
297 the frost layer. For scenarios with solid frost layers (Figure 2), water is initially lost from the
298 near-surface of the “water conserving” peat via evaporation (Figure 2); within the near
299 surface the volumetric water content (VWC, θ) declines to ~ 0.26 after three days (Figure 2a)
300 and quickly raises near-surface tensions limiting evaporation. As a result, after a week of
301 evaporation, VMC in the top 0.05 m of peat profile is low (Figures 2a and 2b). However, the
302 water table did not drop below 0.10 m until day 26 (VWC equals the saturated water content
303 of $\theta_s = 0.94$; Figure 2c), with a saturated zone remaining above the frozen layer (Figure 2d; $\theta =$
304 θ_s). In comparison, for “productive” combinations of peat hydraulic properties, surface
305 tensions did not rise to levels that limit evaporation. Profiles thus continued to evaporate
306 and the water table dropped to the depth of the frozen layer on day seven of the simulation



307
308 Figure 2 –Volumetric Water Content over time for solid frozen soil layer at 0.20 m
309 depth. Different panels show VWC at different depths in the peat profile for three
310 different set of peat hydraulic properties; productive, mean and water conserving.

311

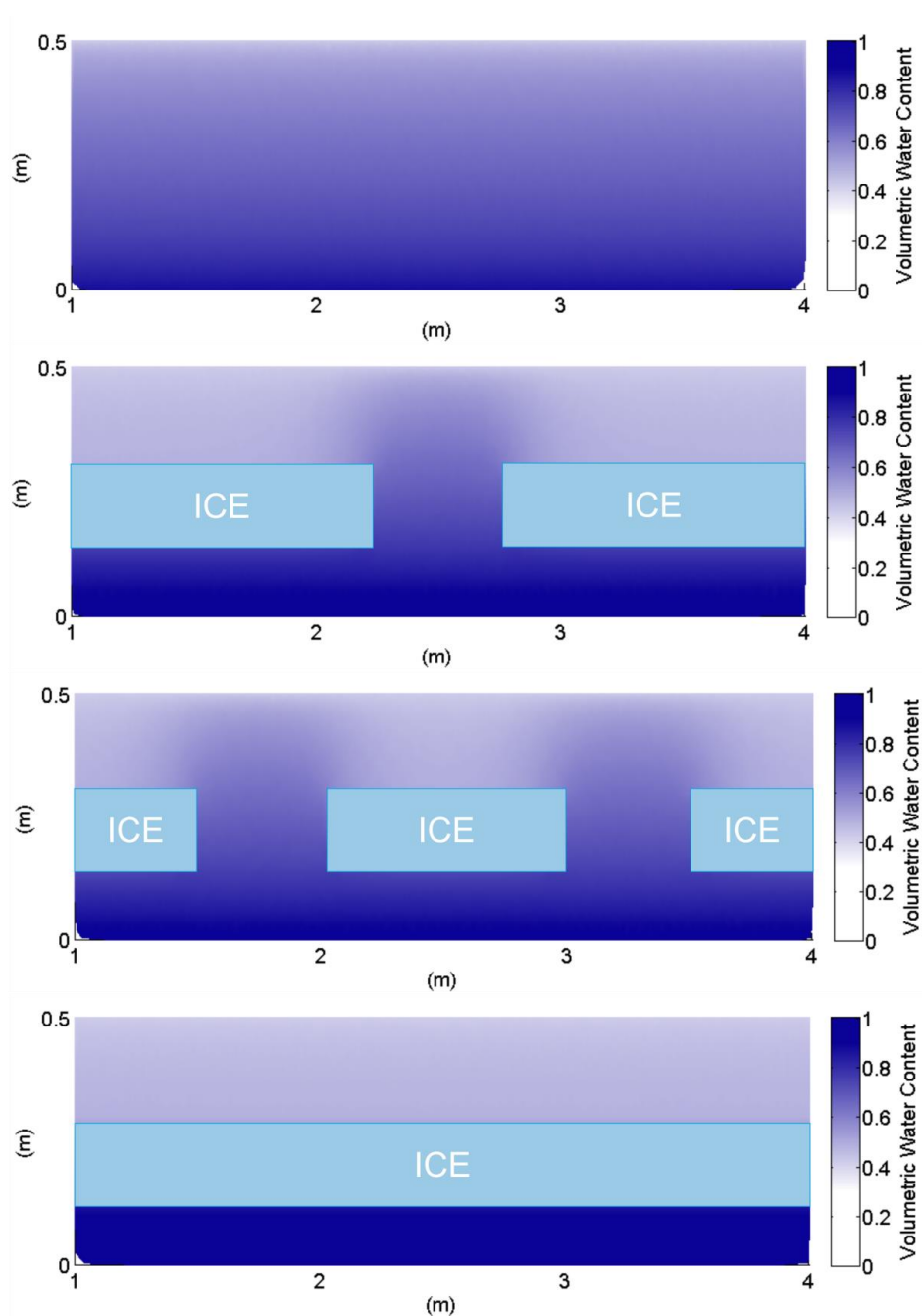


312 (Figure 2d; VWC declined after day 7). Thereafter, the VWC in the peat layer above the frost
313 layer continues to decline, as evaporation is sourced from unsaturated zone storage above
314 the frost layer. After three weeks of evaporation, the VMC at 0.15 m depth is less than 0.50
315 (Figure 2d).

316 For scenarios with one or more holes in the frost layer, simulated VMC for the mean and
317 water conservation hydraulic properties are the same as for the solid frost layer. This is
318 because the water table does not drop to the depth of the frost layer during simulations.
319 Therefore, continuity in the frost layer is only important for “productive peat” scenarios
320 (Figure 3). For productive peat, holes in the frost layer result in spatiotemporal variations in
321 water contents and tensions as water is transported to the surface from the saturated peat
322 below the discontinuous frost layer (Figure 3b/c). Once the water table drops below the
323 level of the frost layer, the near-surface peat over a hole in the frost layer is able to maintain
324 a VWC of $\theta \approx 0.50$. However, within the vadose zone, lateral transfer of water supplied
325 through the gap is very limited (Figure 3bc). After five weeks of evaporation there is a clear
326 difference in near-surface VWC between the frozen soil scenarios (Figure 3). The frost free
327 (Figure 3a) and solid frost (Figure 3d) scenarios represent the two extremes in VWC, with
328 the discontinuous frost layer scenarios (Figures 3b/c) showing characteristics of both solid
329 frost and frost free scenarios. Where there is a break in the frozen layer, VWC immediately
330 above the break corresponds to the frost free scenario (Figure 3a). However, a short lateral
331 distance away from the break the VWC in the discontinuous frost scenarios closely
332 resembles the solid frost scenario (Figure 3d).

333 Once the water table has reached the depth of the frost layer the near-surface peat above the
334 layer does not replace water lost through evaporation and thus peat VWC continues to
335 decline until near-surface water tensions reach 400 mb and evaporation is limited.
336 Conversely, above the breaks in the frost layer the near-surface water tensions remain in the
337 range 150-350 mb over the whole diurnal cycle, indicating that water supplied from deeper
338 saturated peat is able to maintain some evaporation. Consequently, discontinuous frost
339 layers generate heterogeneity in near-surface VWC; $\theta \approx 0.60$ above breaks in the frozen layer
340 compared to $\theta \approx 0.45$ above the frozen layer (Figures 3b and 3c).

341



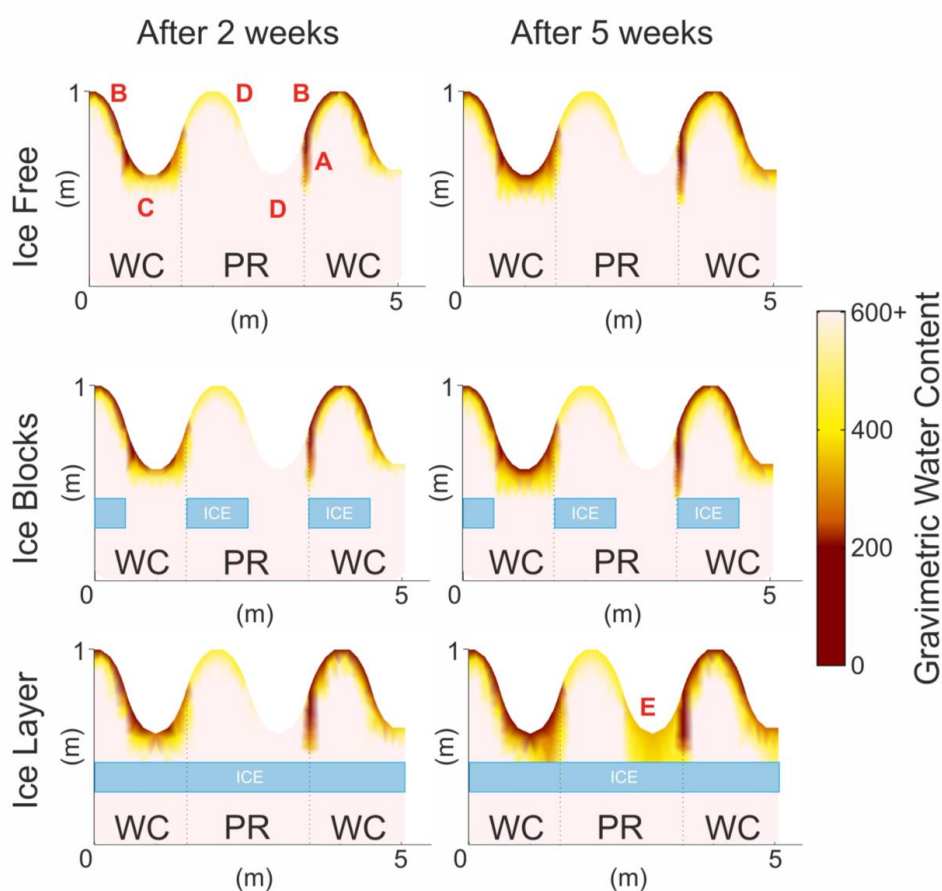
342
343
344
345
346
347

Figure 3 – Water balance in four different frost layer model scenarios after five weeks of diurnal evaporation. This shows breaks in the frost layer allow the evaporating surface to maintain connectivity to the falling water table below the ice, but there is limited lateral connectivity with little water supplied to areas not directly above the hole.



348 **3.3 2-D model simulations (topography included)**

349 Hummock-hollow microtopography simulations show lateral water transfer between
 350 adjacent water conserving and productive zones that substantially influences GWC and
 351 associated wildfire severity. Although the spatial extent of lateral water transfer is limited,
 352 and its influence doesn't extend beyond 0.5 m, this can induce strong spatial variability in



353
 354
 355
 356
 357
 358
 359
 360
 361
 362
 363

Figure 4 – Gravimetric water contents across modelled domains after two and five weeks of evaporation. WC = Water conserving peat type, PR = Productive peat type. The water table intersects the frost layer on day 26, as a result there are only minimal differences in water content distributions between the different ice scenarios after two weeks. For the results after five weeks, where the water table is below the level of the frost layer, the surface moisture content is partly determined by connectivity to the falling water table. This shows productive areas above solid ice will dry out substantially compared to the same areas over discontinuous or absent frost layers (See text for discussion of labels A-D).



364 GWC (Figure 4). Lateral water transfer results in zones of low GWC typically at the sides of
365 peat hummocks (one example labelled as “A” in Figure 4). These represent zones of high
366 susceptibility to deep smouldering combustion and thus high burn severity.

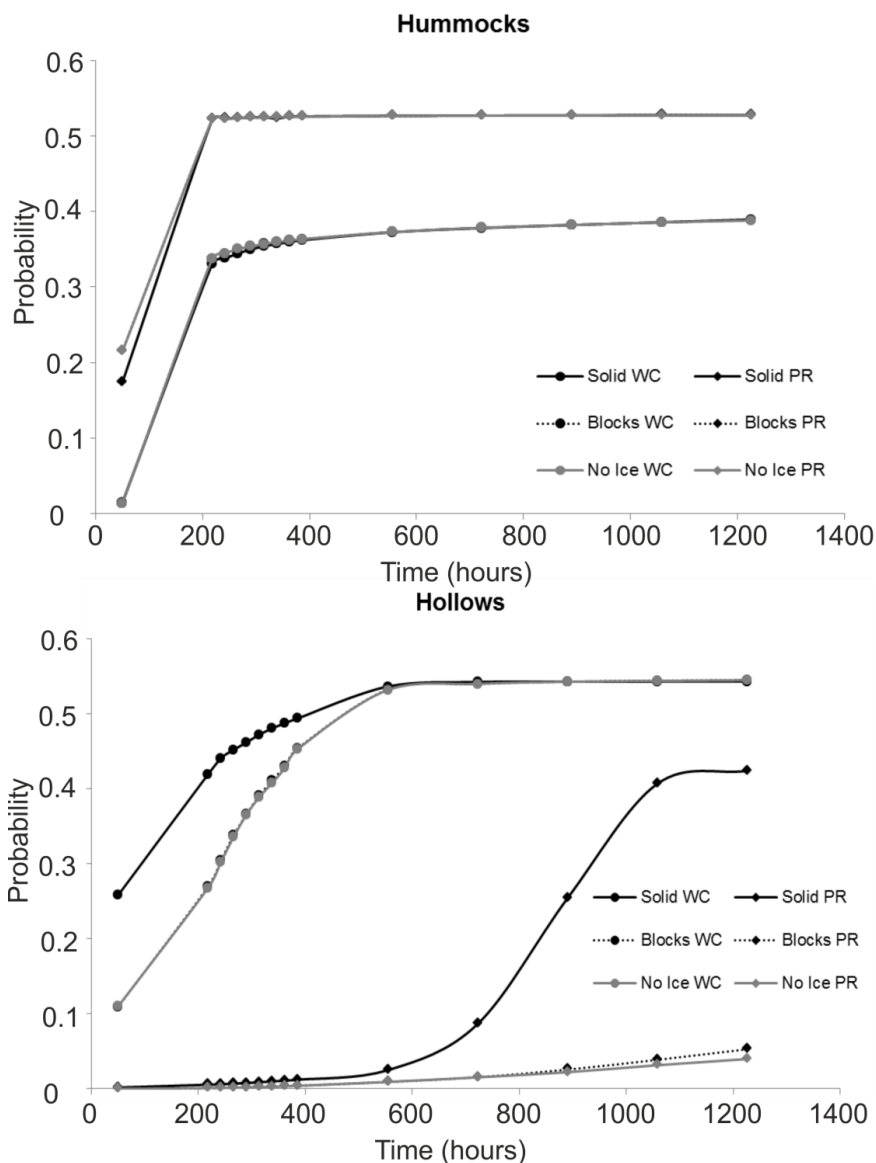
367 Evaporation and GWCs of a given profile through the transect depends both on the
368 hydraulic properties of the profile itself, and the hydraulic properties of adjacent areas. After
369 two weeks of evaporation, the water table has not declined to the depth of the frost layer,
370 thus the ice and ice-free scenarios behave similarly (Figure 4a/b). Areas of water conserving
371 peat, which respond to evaporative stress with high surface tensions, have very low near-
372 surface GWCs. As such, water conserving hummocks exhibit GWCs <250 % at depths of
373 <0.03 m (e.g. “B” in Figure 4). Similarly hollows have GWCs <250% to a depth of 0.05m (e.g.
374 “C” in Figure 4). At depth within both hummocks and hollows, deeper peat has much
375 higher GWC. Conversely, areas with productive peat facilitate the upwards movement of
376 water from deeper in the peat, resulting in a more even vertical distribution of GWC (e.g.
377 “D” in Figure 4). This results in higher GWC at the near-surface of productive hummocks
378 compared to water conserving hummocks. In productive hollows, this results in higher
379 water contents at the near-surface and lower water contents at depth.

380 Five weeks into the simulation, GWC varies little between the frost free and broken frost
381 layer scenarios (Figure 4); however, the scenario with a solid frost layer, shows that the
382 GWCs of hollows are substantially lower compared to the other ice scenarios and the same
383 ice scenario after three weeks (Figure 4). In productive hollows, after five weeks (labelled
384 “E” in Figure 4), the surface GWC is 400%, compared 800% for the no ice scenario. In water
385 conserving hollows surface water contents are similar for all ice scenarios.

386 Interactions between adjacent water conserving and productive areas create small regions of
387 enhanced heterogeneity in GWC (labelled “A” in Figure 4). In the case of a water conserving
388 hummock next to a productive hollow, water is drawn out of the side of the hummock and a
389 region of very low GWC develops at the margin of the water conserving area. This region of
390 low GWC is affected by the presence of a solid frost layer, with the area being slightly larger
391 for the solid ice scenario compared to the other two scenarios after three weeks and
392 substantially larger and also of much lower GWCs after five weeks (Figure 4).



393 3.4 Differences between microtopographic position and hydraulic properties

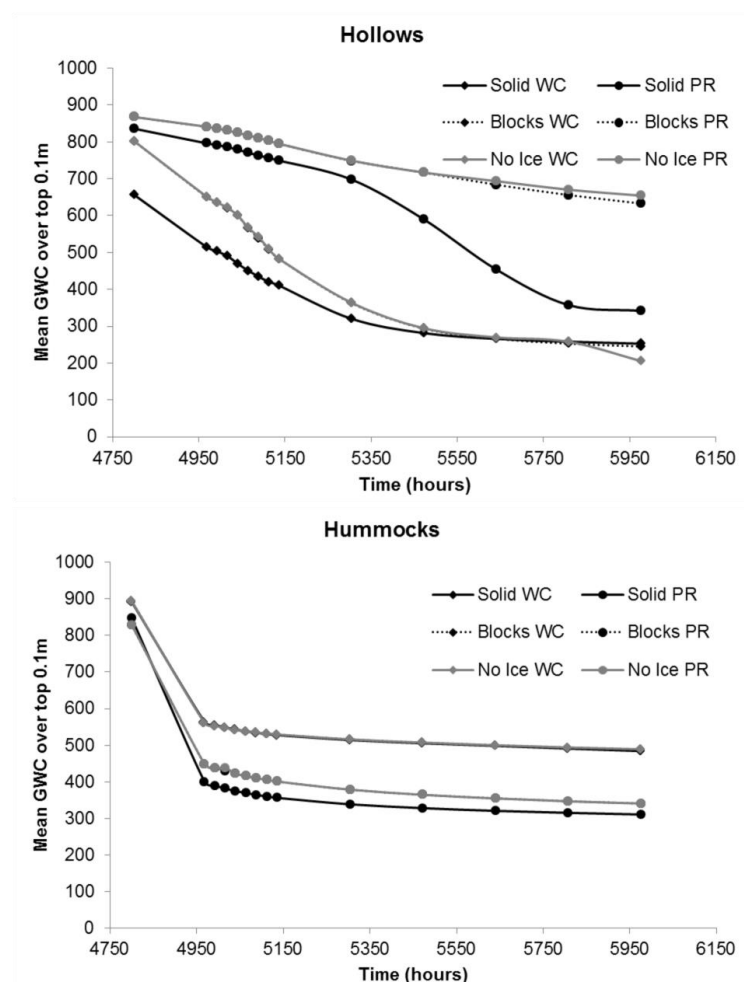


394
 395 Figure 5 – The probability of ignition (gravimetric water content is lower than
 396 250%), for near-surface peat, over time for the different microtopographic areas
 397 and hydraulic properties (PR – Productive peat properties, WC – Water conserving
 398 peat properties)

399 For hummocks, all scenarios show very little change in surface water content over the model
 400 runs and show little difference between scenarios (Figure 4), a finding which is shown
 401 quantitatively in Figure 5A. Probabilistic GWCs are calculated based on the normal



402 distribution of peat densities using Eq. (8). Results are displayed as the probability of GWC
 403 being lower than 250%, representing a threshold for smouldering. All scenarios show similar
 404 hummock probabilities over time for both hydraulic properties types (Figure 5A), indicating
 405 the presence of a solid frost layer has only a small influence on hummock GWC. Conversely
 406 solid ice has a substantial effect on hollow GWC (Figure 5B). In productive peat hollows
 407 probabilities rise steeply two weeks into the simulation and the ice free and ice block



408

409 Figure 6 – Mean gravimetric water content over the top 0.1m of the profile for
 410 different microtopographic features showing how vulnerability to deeper
 411 smouldering varies over time for different scenarios and features.

412 scenarios diverge (Figure 5B). Mean GWC over the top 0.10 m of the peat profile (Figure 6)

413 shows a similar pattern to Figure 5. Hummock GWC is relatively insensitive to ice scenario,



414 whereas for hollows the solid ice scenario shows generally lower GWC over the top 0.1m
415 compared to other scenarios (Figure 6A).

416 4. Discussion

417 Our results show that seasonal frost layers can affect near-surface GWC and thus the
418 vulnerability of peat to smouldering during wildfires. However, this increased vulnerability
419 probability is also dependent on peat hydrological properties and microtopographical
420 position.

421 4.1 Peatland vadose zone hydrology in presence of ice

422 In common with other studies, numerical modelling herein demonstrates that peat hydraulic
423 properties exert a primary control on near-surface water contents (Kettridge et al.,
424 2015a; McCarter and Price, 2014; Dixon et al., 2017). Notably, simulations indicate presence or
425 absence of a frost layer has a minimal effect on the water balance for peat hydraulic
426 properties which restrict the unsaturated water flow, and thus limit evaporation (*water*
427 *conserving*). In such case, a drier near-surface peat layer developed with volumetric water
428 contents of $\theta=0.30-0.50$ in the upper 0.05 m. However, below 0.10 m depth, peat remained
429 saturated over multiple weeks of evaporation (Figure 2). Therefore, even after six weeks of
430 evaporation, the water table remains at a depth no greater than 0.15m, which is higher than
431 the observed spring depth of ice in boreal peatlands (Figure 2, and Petrone et al., 2008).
432 Conversely, for peats that facilitate unsaturated water flow from depth to the evaporating
433 surface (*productive*), ice has a substantial effect on water contents. Although productive peat
434 readily supplies water to the evaporating surface and maintains a wetter near-surface
435 (Figure 2), greater evaporation, compared to water conserving peat, drove a rapid fall in the
436 water table and, subsequently lowered water contents at depth. In situations where
437 productive peat is underlain by a solid frost layer, the water table dropped to the level of the
438 ice, and subsequently the peat above of the frost layer continued to dry out with further
439 evaporation (Figure 3). Although surface tensions rose during drying in the layer above the
440 ice these did not become high enough to begin to limit evaporation until the peat at 0.15m
441 depth had a water content of $\theta=0.60$ and evaporation persisted even with $\theta=0.45$.

442

443 Horizontal gaps in the frost layer allow the evaporating surface to maintain hydrological
444 connectivity with the falling water table and thus avoid *productive* peat drying out (Figures 2



445 and 4). However, the primary unsaturated flow direction from depth is vertical and there is
446 limited lateral flow away from the frost gap. This results in heterogeneity of near-surface
447 water contents with areas directly above the frost gap maintaining near-surface water
448 contents similar to frost free scenarios, whereas more distant areas dry out to the same
449 extent as solid frost layer scenarios (Figures 2 and 3).

450

451 Where peat hydraulic properties are varied across a hummock-hollow microtopography
452 sequence water balance patterns become more complex compared to a planar atmospheric
453 boundary (Figure 3). As with a flat atmospheric boundary, *water conserving* hollows are
454 characterised by a very dry near-surface (upper 0.05 m), but with much higher water
455 contents at depths of greater than 0.1 m. Conversely, *productive* hollows are able to maintain
456 high near-surface volumetric water contents and maintain hydrological connectivity with a
457 falling water table. As with the planar surface scenarios the transfer of water from depth
458 through the frost gap is primarily vertical, with little lateral transfer of water away from the
459 gap. The combination of a discontinuous frost layer with variations in peat hydraulic
460 properties across a hummock-hollow microtopography leads to a high degree of
461 heterogeneity in volumetric and gravimetric water contents.

462

463 It is important to note however that our initial model conditions assume near saturation
464 following spring snow melt above the frost layer. The system is thus relatively wet, with a
465 shallow starting water table. A drier set of initial conditions, either as a result of different
466 hydrogeological conditions, a drier autumn period leaving the soil drier before winter, or a
467 smaller snowmelt recharge, would mean a lower starting water table and, therefore, an
468 increased probability that the water table will reach the frost layer, as observed by *Petrone et*
469 *al* [2008]. We also assume the frost layer does not thaw during the model runs and thus does
470 not provide water recharge, which is calculated as approximately 1.8 mm/day. We assume a
471 fixed daily evaporation rate of 4.5 mm/day; this is a fairly high rate, however, *Sphagnum*
472 evapotranspiration rates can reach an average of 0.47 mm/hr, and unlike systems which
473 show highest ET rates coincident with highest air temperatures, Alberta peatlands show
474 peak ET rates during the early growing season as frozen soil is thawing (Brown et al., 2010),
475 which is the period being modelled. Finally, the critical surface tension threshold (h_{critA})



476 which shuts off evaporation, here a fixed value of 400mb after McCarter and Price (2014),
477 needs to be considered. It is reasonable to assume the true value of h_{critA} will vary with
478 relative humidity and may in fact be higher at some points during the model runs which
479 represent prolonged rain free periods. As a result, the model scenarios may underestimate
480 total evaporation, but overestimate the drying given the lack of thawing frost recharge.
481 However, all these assumptions (no thaw, evaporation rate, h_{critA} and initial conditions) are
482 within 1-2 mm/day, and are constant between scenarios.

483

484 Considering these assumptions, we restrict ourselves to exploring relative comparisons in
485 VWC and GWC between the modelling scenarios, rather than use modelling results to
486 deliver quantitative predictions. The overall effect of our modelling assumptions is likely to
487 mean that for a given real peatland the time taken to reach a given point in the results may
488 be under or overestimated, but the overall pattern of behaviour is likely to be consistent as
489 this is governed by the peat hydrological properties. If more water is lost through
490 evaporation (higher evaporation rate or dynamic H_{critA}), or the initial conditions are drier,
491 then the water table will recede to a deeper level earlier and the near-surface GWCs will fall
492 earlier. Conversely, if the recharge from thawing frost is accounted for under the same
493 evaporative and initial conditions the water table recession will be slower and it will take
494 longer for the near-surface GWCs to fall.

495

496 ***4.2 Implications for peatland wildfire burn severity***

497 Our results suggest that seasonal frost has a pronounced effect on potential burn depths in
498 boreal peatlands during periods of pronounced drying. Regardless of the type of peat
499 properties, the frost table makes near-surface peat layers, particularly in hollows, more
500 vulnerable to wildfire (smouldering) following a multi-week period without rain by
501 reducing near-surface moisture contents. Given that burn severity in peatlands is highly
502 heterogeneous (Lukenbach et al., 2016), seasonal frost dynamics along with peat hydraulic
503 properties may help explain why some hummocks (or hollows) burn more severely than
504 others. Specifically, the uneven thawing of ice in spring may drive heterogeneity in
505 connectivity to the water table and facilitate variations in near-surface GWC. Pronounced
506 variability in burn severity within microform types has been observed (Lukenbach et al.,



507 2015a, 2016), and these results illustrate hydrological mechanisms beyond peat properties
508 which can drive variability in the probability of peat ignition during wildfire.

509

510 The probability that gravimetric water contents are lower than a critical smouldering
511 threshold of ~250% (c.f. Thompson et al., 2015; Zoltai et al., 1998; Lukenbach et al.,
512 2015b; Benscoter et al., 2011) are higher when a frost layer was present compared to when it
513 was absent, and was most pronounced for areas with productive peat hydraulic properties
514 (Figures 5). The most sensitive sub-set is productive hollows, where the presence of a frost
515 layer substantially increases the probability that near-surface GWC drops below 250%
516 (Figure 5) and also lowers the average GWC over the top 0.1m of the profile (Figure 6). Our
517 results indicate that ice free conditions coinciding with a prolonged rain free period in
518 peatland would result in approximately 50% of hummocks being vulnerable to smouldering
519 combustion (Figure 5A), with approximately 25% of hollows vulnerable to smouldering
520 combustion and potentially deep depths of burn (Figure 5B). In the presence of a solid frost
521 layer, however, the proportion of hollows vulnerable to appreciable smouldering depths
522 rises to around 50% (Figure 6B), effectively doubling the extent of deeper depth of burn.
523 Heightened heterogeneity in water content can occur when adjacent areas have different
524 hydraulic properties. A wedge of low GWC develops where either a water conserving
525 hummock is next to a productive hollow, or a productive hummock is adjacent to a water
526 conserving hollow (labelled as “A” in Figure 4). Results also indicate that although
527 hummocks are much higher above the water table, they are able to retain a moist vadose
528 zone (e.g. Benscoter and Wieder, 2003; Thompson and Waddington, 2013; Shetler et al.,
529 2008; Lukenbach et al., 2015b; Benscoter et al., 2011) and are to an extent hydrologically
530 disconnected from the water table with surface water balance dependant on water retained
531 within the hummock; this means they are characterised by a very dry near-surface, but a
532 moist enough interior of the hummock that GWCs offer protection against deep
533 smouldering, regardless of the presence or absence of a frost layer.

534

535 An interesting implication of these results is that productive hummocks may be better able
536 to maintain higher near-surface GWCs and thus resist smouldering combustion; this would
537 mean that they are better placed to recover quickly from wildfires (Lukenbach et al., 2015a,



538 2016). Conversely, more water conserving hummocks may be susceptible to higher burn
539 severity due to their very dry near-surface, and may then be unable to recover quickly post-
540 fire or continue to conserve water (Lukenbach et al., 2016, 2015a). The presence of seasonal
541 frost layers changes the implications of burn severity and recovery and introduces a trade
542 off in the optimum peat profiles. For hollows, a water conserving peat would be slower
543 growing and experience more frequent periods of water stress, however when ice is present
544 it will be characterised by a thin, dry layer above a relatively moist layer which may restrict
545 smouldering to a thin surface band of peat and promote more rapid recovery post-fire.
546 Conversely, hollows with productive peat will be able to buffer periods of water stress and
547 will be faster growing, however, they will be vulnerable to drying out in the presence of a
548 frost layer, meaning they could be subject to high burn severity and then take a long time to
549 subsequently recover ecohydrological function.

550 5. Conclusions

551 Two dimensional numerical modelling results show that seasonal frost layers can play an
552 important role in disconnecting the evaporating surface of the peatland from the deeper
553 water table and so can enhance heterogeneity in near-surface water contents, which likely
554 influences patterns of ignition and burn severity during wildfire. In common with other
555 studies, we find peat hydraulic properties provide an important control on peat water
556 balance, as they control the ability of the peat to transmit water from deeper saturated layers
557 to the evaporating surface. Hummock microforms are typically higher above the water table
558 and so over seasonal timescales do not depend on direct connection to the deep water table
559 to supply evaporative demand, rather they utilise water stored in a large unsaturated mass
560 of the hummock. As a result of their decreased dependence on connection to the water table,
561 hummock microforms are relatively unaffected by the presence of a seasonal frost layer.
562 Conversely, hollow microforms depend to a greater degree on maintaining connectivity to
563 the water table in order to supply water to meet evaporative demand. Hollows which tend
564 towards water conserving are less able to transmit water from deeper saturated layers will
565 tend to dry out at the very near-surface, but maintain high tensions and pressure gradients
566 to layers with higher water contents immediately below. In prolonged rain free periods,
567 regardless of seasonal ice presence, these areas are therefore vulnerable to deep smouldering
568 in wildfire. Conversely, hollows comprised of peat which tends towards greater production



569 and water use, are highly dependent on seasonal ice presence. Productive hollows will dry
570 out in the presence of a seasonal frost layer as their surface is disconnected from the water
571 table. In addition, they are able to maintain productivity, and evaporation, in the presence of
572 low water contents, and therefore can be subjected to substantial drying. This substantial
573 drying will make the area vulnerable to deep burning in wildfires. At the landscape scale
574 our results show the presence of a frost layer with a prolonged rain free period will increase
575 the proportion of hollows vulnerable to deeper burning (>0.1 m) from 25% to 50%. The high
576 degree of natural variability in peat hydraulic properties will lead to a high degree of
577 heterogeneity in near-surface water contents during rain free periods, and thus
578 heterogeneity in wildfire burning within microform type. The presence of a seasonal frost
579 layer both raises the overall risk of smouldering and deeper burning (>0.1 m) during
580 wildfires, but also enhances the degree of heterogeneity.



- 581 Baird, A. J., Eades, P. A., and Surridge, B. W. J.: The hydraulic structure of a raised bog
582 and its implications for ecohydrological modelling of bog development, *Ecohydrology*, 1,
583 289-298, 2008.
- 584 Baird, A. J., Milner, A. M., Blundell, A., Swindles, G. T., and Morris, P. J.: Microform-
585 scale variations in peatland permeability and their ecohydrological implications, *Journal of*
586 *Ecology*, 104, 531-544, 10.1111/1365-2745.12530, 2016.
- 587 Beckwith, C. W., Baird, A. J., and Heathwaite, A. L.: Anisotropy and depth - related
588 heterogeneity of hydraulic conductivity in a bog peat. I: laboratory measurements,
589 *Hydrological processes*, 17, 89-101, 2003.
- 590 Bencotter, B. W., and Wieder, R. K.: Variability in organic matter lost by combustion in
591 a boreal bog during the 2001 Chisholm fire, *Canadian Journal of Forest Research*, 33, 2509-
592 2513, 10.1139/x03-162, 2003.
- 593 Bencotter, B. W., Thompson, D. K., Waddington, J. M., Flannigan, M. D., Wotton, B.
594 M., De Groot, W. J., and Turetsky, M. R.: Interactive effects of vegetation, soil moisture and
595 bulk density on depth of burning of thick organic soils, *International Journal of Wildland*
596 *Fire*, 20, 418-429, 2011.
- 597 Boelter, D. H.: Hydraulic conductivity of peats, *Soil Science*, 100, 227-231, 1965.
- 598 Branham, J. E., and Strack, M.: Saturated hydraulic conductivity in Sphagnum -
599 dominated peatlands: do microforms matter?, *Hydrological Processes*, 28, 4352-4362, 2014.
- 600 Brown, S. M., Petrone, R. M., Mendoza, C., and Devito, K. J.: Surface vegetation
601 controls on evapotranspiration from a sub - humid Western Boreal Plain wetland,
602 *Hydrological Processes*, 24, 1072-1085, 10.1002/hyp.7569, 2010.
- 603 Devito, K. J., Mendoza, C. A., and Qualizza, C.: Conceptualizing water movement in
604 the Boreal Plains. Implications for watershed reconstruction. Synthesis report prepared for
605 the Canadian Oil Sands Network for Research and Development, Environmental and
606 Reclamation Research Group, 164, 2012.
- 607 Dixon, S. J., Kettridge, N., Moore, P. A., Devito, K. J., Tilak, A. S., Petrone, R. M.,
608 Mendoza, C. A., and Waddington, J. M.: Peat depth as a control on moss water availability
609 under evaporative stress, *Hydrological Processes*, 31, 4107-4121, 10.1002/hyp.11307, 2017.
- 610 Flannigan, M. D., Logan, K. A., Amiro, B. D., Skinner, W. R., and Stocks, B.: Future
611 area burned in Canada, *Climatic change*, 72, 1-16, 2005.



- 612 Frolking, S., and Roulet, N. T.: Holocene radiative forcing impact of northern peatland
613 carbon accumulation and methane emissions, *Global Change Biology*, 13, 1079-1088, 2007.
- 614 Gorham, E.: Northern peatlands: role in the carbon cycle and probable responses to
615 climatic warming, *Ecological applications*, 1, 182-195, 1991.
- 616 Hogan, J. M., Van der Kamp, G., Barbour, S. L., and Schmidt, R.: Field methods for
617 measuring hydraulic properties of peat deposits, *Hydrological processes*, 20, 3635-3649,
618 2006.
- 619 Hokanson, K. J., Lukenbach, M. C., Devito, K. J., Kettridge, N., Petrone, R. M., and
620 Waddington, J. M.: Groundwater connectivity controls peat burn severity in the boreal
621 plains, *Ecohydrology*, 9, 574-584, [10.1002/eco.1657](https://doi.org/10.1002/eco.1657), 2016.
- 622 Kasischke, E. S., and Turetsky, M. R.: Recent changes in the fire regime across the
623 North American boreal region—spatial and temporal patterns of burning across Canada and
624 Alaska, *Geophysical research letters*, 33, 2006.
- 625 Kennedy, G. W., and Price, J. S.: A conceptual model of volume-change controls on the
626 hydrology of cutover peats, *Journal of Hydrology*, 302, 13-27, 2005.
- 627 Kettridge, N., Tilak, A. S., Devito, K. J., Petrone, R. M., Mendoza, C. A., and
628 Waddington, J. M.: Moss and peat hydraulic properties are optimized to maximize peatland
629 water use efficiency, *Ecohydrology*, 2015a.
- 630 Kettridge, N., Turetsky, M. R., Sherwood, J. H., Thompson, D. K., Miller, C. A.,
631 Benscoter, B. W., Flannigan, M. D., Wotton, B. M., and Waddington, J. M.: Moderate drop in
632 water table increases peatland vulnerability to post-fire regime shift, *Scientific reports*, 5,
633 2015b.
- 634 Lewis, C., Albertson, J., Xu, X., and Kiely, G.: Spatial variability of hydraulic
635 conductivity and bulk density along a blanket peatland hillslope, *Hydrological Processes*,
636 26, 1527-1537, [10.1002/hyp.8252](https://doi.org/10.1002/hyp.8252), 2012.
- 637 Lukenbach, M. C., Devito, K. J., Kettridge, N., Petrone, R. M., and Waddington, J. M.:
638 Hydrogeological controls on post-fire moss recovery in peatlands, *Journal of Hydrology*,
639 530, 405-418, <http://dx.doi.org/10.1016/j.jhydrol.2015.09.075>, 2015a.
- 640 Lukenbach, M. C., Hokanson, K. J., Moore, P. A., Devito, K. J., Kettridge, N.,
641 Thompson, D. K., Wotton, B. M., Petrone, R. M., and Waddington, J. M.: Hydrological



- 642 controls on deep burning in a northern forested peatland, *Hydrological Processes*, 29, 4114-
643 4124, 10.1002/hyp.10440, 2015b.
- 644 Lukenbach, M. C., Devito, K. J., Kettridge, N., Petrone, R. M., and Waddington, J. M.:
645 Burn severity alters peatland moss water availability: Implications for post-fire recovery,
646 *Ecohydrology*, 9, 341-353, 2016.
- 647 McCarter, C. P. R., and Price, J. S.: Ecohydrology of Sphagnum moss hummocks:
648 mechanisms of capitula water supply and simulated effects of evaporation, *Ecohydrology*, 7,
649 33-44, 2014.
- 650 McCauley, C. A., White, D. M., Lilly, M. R., and Nyman, D. M.: A comparison of
651 hydraulic conductivities, permeabilities and infiltration rates in frozen and unfrozen soils,
652 *Cold Regions Science and Technology*, 34, 117-125, [http://dx.doi.org/10.1016-](http://dx.doi.org/10.1016/S0165-232X(01)00064-7)
653 [232X\(01\)00064-7](http://dx.doi.org/10.1016/S0165-232X(01)00064-7), 2002.
- 654 Petrone, R. M., Devito, K. J., Silins, U., Mendoza, C. A., Brown, S. C., Kaufman, S. C.,
655 and Price, J. S.: Transient peat properties in two pond-peatland complexes in the sub-humid
656 Western Boreal Plain, Canada, *Mires & Peat*, 3, 2008.
- 657 Prat-Guitart, N., Rein, G., Hadden, R. M., Belcher, C. M., and Yearsley, J. M.:
658 Propagation probability and spread rates of self-sustained smouldering fires under
659 controlled moisture content and bulk density conditions, *International Journal of Wildland*
660 *Fire*, 25, 456-465, <https://doi.org/10.1071/WF15103>, 2016.
- 661 Quinton, W. L., Hayashi, M., and Carey, S. K.: Peat hydraulic conductivity in cold
662 regions and its relation to pore size and geometry, *Hydrological Processes*, 22, 2829-2837,
663 10.1002/hyp.7027, 2008.
- 664 Roulet, N., Moore, T., Bubier, J., and Lafleur, P.: Northern fens: methane flux and
665 climatic change, *Tellus B*, 44, 100-105, 1992.
- 666 Sherwood, J. H., Kettridge, N., Thompson, D. K., Morris, P. J., Silins, U., and
667 Waddington, J. M.: Effect of drainage and wildfire on peat hydrophysical properties,
668 *Hydrological Processes*, 27, 1866-1874, 2013.
- 669 Shetler, G., Turetsky, M. R., Kane, E. S., and Kasischke, E. S.: Sphagnum mosses limit
670 total carbon consumption during fire in Alaskan black spruce forests, *Canadian Journal of*
671 *Forest Research*, 38, 2328-2336, 2008.



- 672 Šimůnek, J., Šejna, M., and Van Genuchten, M. T.: The HYDRUS-2D software package
673 for simulating the two-dimensional movement of water, heat, and multiple solutes in
674 variably-saturated media: version 2.0, US Salinity Laboratory, Agricultural Research Service,
675 US Department of Agriculture, 1999.
- 676 Smith, L. C., MacDonald, G. M., Velichko, A. A., Beilman, D. W., Borisova, O. K., Frey,
677 K. E., Kremenetski, K. V., and Sheng, Y.: Siberian peatlands a net carbon sink and global
678 methane source since the early Holocene, *Science*, 303, 353-356, 2004.
- 679 Stocks, B. J., Mason, J. A., Todd, J. B., Bosch, E. M., Wotton, B. M., Amiro, B. D.,
680 Flannigan, M. D., Hirsch, K. G., Logan, K. A., and Martell, D. L.: Large forest fires in Canada,
681 1959–1997, *Journal of Geophysical Research: Atmospheres*, 107, 2002.
- 682 Thompson, D. K., and Waddington, J. M.: Wildfire effects on vadose zone hydrology
683 in forested boreal peatland microforms, *Journal of hydrology*, 486, 48-56, 2013.
- 684 Thompson, D. K., Wotton, B. M., and Waddington, J. M.: Estimating the heat transfer
685 to an organic soil surface during crown fire, *International Journal of Wildland Fire*, 24, 120-
686 129, 2015.
- 687 Turetsky, M. R., Wieder, K., Halsey, L., and Vitt, D.: Current disturbance and the
688 diminishing peatland carbon sink, *Geophysical Research Letters*, 29, 2002.
- 689 Turetsky, M. R., Amiro, B. D., Bosch, E., and Bhatti, J. S.: Historical burn area in
690 western Canadian peatlands and its relationship to fire weather indices, *Global
691 Biogeochemical Cycles*, 18, 2004.
- 692 Turetsky, M. R., Kane, E. S., Harden, J. W., Ottmar, R. D., Manies, K. L., Hoy, E., and
693 Kasischke, E. S.: Recent acceleration of biomass burning and carbon losses in Alaskan forests
694 and peatlands, *Nature Geoscience*, 4, 27-31, 2011.
- 695 Van Genuchten, M. T.: A closed-form equation for predicting the hydraulic
696 conductivity of unsaturated soils, *Soil science society of America journal*, 44, 892-898, 1980.
- 697 Wieder, R. K., Scott, K. D., Kamminga, K., Vile, M. A., Vitt, D. H., Bone, T., Xu, B.,
698 Benscoter, B. W., and Bhatti, J. S.: Postfire carbon balance in boreal bogs of Alberta, Canada,
699 *Global Change Biology*, 15, 63-81, 2009.
- 700 Yu, Z., Loisel, J., Brosseau, D. P., Beilman, D. W., and Hunt, S. J.: Global peatland
701 dynamics since the Last Glacial Maximum, *Geophysical Research Letters*, 37, 2010.



702 Zoltai, S. C., Morrissey, L. A., Livingston, G. P., and Groot, W. J.: Effects of fires on
703 carbon cycling in North American boreal peatlands, *Environmental Reviews*, 6, 13-24,
704 10.1139/a98-002, 1998.

705